The impact resistance of concrete slabs under heavy dropped loads

A.C.E.Sinclair & K.Fullard
CEGB Berkeley Nuclear Laboratories, Gloucestershire, UK
D.Baker
CEGB Structural Test Centre, Cheddar, Somerset, UK

ABSTRACT

A series of impact tests has been conducted on large-scale concrete targets, intended to represent floor slabs supported on beams. The results indicate that for very heavy loads the NDRC and CEA/EDF/AEEW formulae commonly used to predict local damage can overestimate the ability of a slab to resist either initial significant damage - here shown to be a through-thickness conical failure - or perforation.

1 INTRODUCTION

The series of tests reported here is part of a programme of studies in the UK designed to establish the resistance of reinforced concrete floor slabs to dropped loads /1/,/2/. The present tests were conducted at the Structural Test Centre of the CEGB, which is equipped to handle the heavy masses required for tests at large scale.

2 EMPIRICAL FORMULAE

Current procedures for predicting local impact damage - scabbing and perforation - are given in /1/. It was recognized that since these were mainly derived from high velocity impacts, their validity required assessment for the low velocities characteristic of dropped loads.

Additionally, most data for perforation had been obtained with targets reinforced symmetrically at front and rear faces whereas our standard targets (as common for floors) had reinforcement only at the <u>rear</u> face. Nevertheless for composite targets, with a steel plate behind the concrete slab, the perforation velocity V_p for a cylinder mass m and diameter d had been properly predicted by

$$(1) \qquad V_p = 1.3\rho^{1/6} f_{cy}^{1/2} \left(\frac{dt^2}{m}\right)^{2/3} (B + 0.3)^{1/2} \qquad \text{(SI units)}$$

where ρ is concrete density, f_{cy} is concrete cylinder strength, t is slab thickness, and B is the simple sum of the quantities, expressed as percentages, of the rear plate steel and the <u>rear</u> face reinforcement. It may be deduced, therefore, that for our slabs eq. (1) applies with B given by the rear face percentage.

3 TEST CONDITIONS

The test parameters were chosen to reflect those of postulated dropped loads on conventional supported floors, at sufficiently large scale that normal commercial concrete and reinforcing steel could be used, and for diameter to thickness ratio > 1. For eq. (1) m = 2500 kg, d = 0.3 or 0.6m, t = 0.3m, B= 0.43%. Internal span was 1.5m (span/thickness = 5.0)

Figure 1 shows a view of the target with ancillary supports.

The standard reinforcement in the impact region, on the rear face only, used high yield bars with 16mm diameter at 150mm pitch (Y16-150 ewrf). Other reinforcement styles were Y12-82 ewrf i.e. thinner bars at closer pitch, giving identical B but allowing us to investigate effects caused by the net mesh and Y16-150 ewef giving standard reinforcement at each face, for comparison purposes with results at higher velocities, where symmetrical reinforcement is usual.

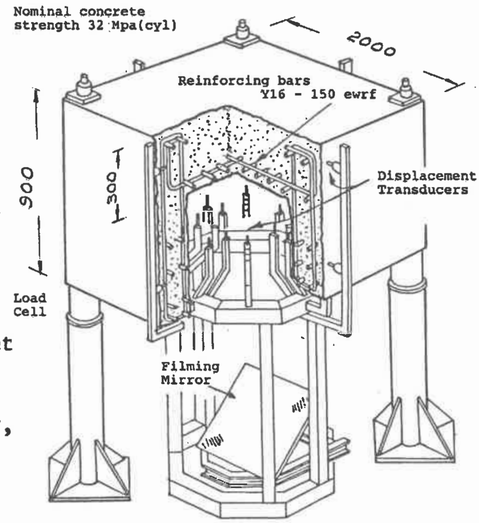

Figure 1 Target arrangement

Three interchangeable noses were used - flat, 176° cone, and 90° cone. The flat nose presented the most severe impact conditions, particularly since accurate drop aligment ensured "flat-on" impacts with 0.2° parellelism between contact faces.

Parallelism of 0.2° is rarely guaranteed in impact testing, so it was important to investigate the shock absorbing effect of a greater offset. The 176° cone mimics a flat face impacting at 2° tilt.

The 90° cone nose allowed us further to examine shock absorption, as for example during the impact of a dropped load falling on a corner.

4 CRITICAL DAMAGE CRITERIA

Two critical damage criteria were sought:

a) Cone cracking, defined by the critical velocity V_{cc} to produce a conical failure surface through the slab thickness, and

b) Perforation, defined by the critical velocity for perforation V_p.

Note that the criterion for first significant damage was not the rear face scabbing which appears in the NDRC formulation. Such scabbing did not necessarily occur even though slab "leak-tightness" was breached.

5 RESULTS AND DISCUSSION

Table I summarises the observations for cone crack formation and for perforation. V_p is derived from impact and exit velocities V_i, V_e through the usual energy balance expression taking account of ejected concrete mass. Also shown are the predictions from the scabbing and perforation formulae. Though as has been noted, the scabbing formula is not truly applicable to the circumstances and observations of the present dropped load impacts, nevertheless, up till now it has been conventionally used as the criterion for avoiding the onset of local damage to structural slabs.

For flat-nosed impacts, the first indication of significant <u>local</u> damage is denoted by a conical failure surface. Both within the contact perimeter and outside, the concrete is undamaged; i.e. the top face of the concrete shows no sign of the crushing implicit in the NDRC formulation. Rather, a solid plug of concrete is knocked on. The impactor is brought to rest at depth h below the surface, the "indentation depth".

Globally, yield cracks are seen on the underside of the target face, running diagonally from the centre towards each corner and down the vertical intersection of the edge beams. Further cracks occur on the beams' inner and outer faces, indicating beam torsion.

5.1 CONE CRACKING

Figure 2 shows sections of four targets after impact near the cone cracking velocity V_{cc}. This critical velocity was derived for the 300mm flat-nosed impactor as V_{cc} = 2.4 m/s. A somewhat higher value, V_{cc}~3.0m/s, is indicated for the 600 mm nose.

It is believed that the cone asymmetry and multiple cracks arose as a result of slight non-parallelism between impactor and impact face. This allowed some small volume of crushing, starting either at an edge or where the top face was slightly humped. The contact region then expanded until it achieved a minimum size, at which instant the conical

Table I Impact results

Nose Shape	Target Reinforcement B=0.43%	Test No.	Concrete Strength f_{cy} MPa	Velocity Impact V_i m/s	Velocity Exit V_e m/s	Indent h mm	Perf. Velocity V_p Test m/s	Perf. Velocity V_p Formula m/s	Deviation of measured V_p from Formula
300mm impactor									
Flat	Y16-150ew rf**	1	44.2	14.1	10.1		9.3	12.1	-23%
		2	39.7	9.0	3.64		8.16	12.1	-33%
		6	35.2	8.0	2.33		7.62	11.8	-35%
		3	42.7	5.0		61			
		4	43.7	4.0		15			
		5	33.0	2.5		0.5			
		For f_{cy} = 32 MPa:							
		Derived critical velocity for cone cracking V_{cc} = 2.4 m/s							
		Predicted critical velocity for NDRC "scabbing" = 5.12 m/s							
		Deviation of V_{cc} from NDRC scabbing = -53%							
176°	" "	18	31.5	9.2	2.44		8.84	11.1	-21%
		17	34.8	8.5		484			
		12	36.2	5.0		31			
		16	31.0	4.0		7			
90°	" "	22	39.3	10.4		174/162			
		19	37.7	5.2		70 (knock-on=15mm)			
Flat	Y12-82ew "	21	35.6	9.5	1.24		9.41	11.85	-21%
"	Y16-150ewef	20	35.7	8.5		142			
600mm impactor									
Flat	Y16-150ewrf	11	27.2	14.0	0*	480*	14.0	16.4	-15%
		9	29.8	12.0		205			
		7	30.5	6.0		34			
		8	33.5	3.7		1.5			
		10	34.5	3.0		0			

* Impactor hooked on broken reinforcing bar.
**rf = rear face, ef = each face

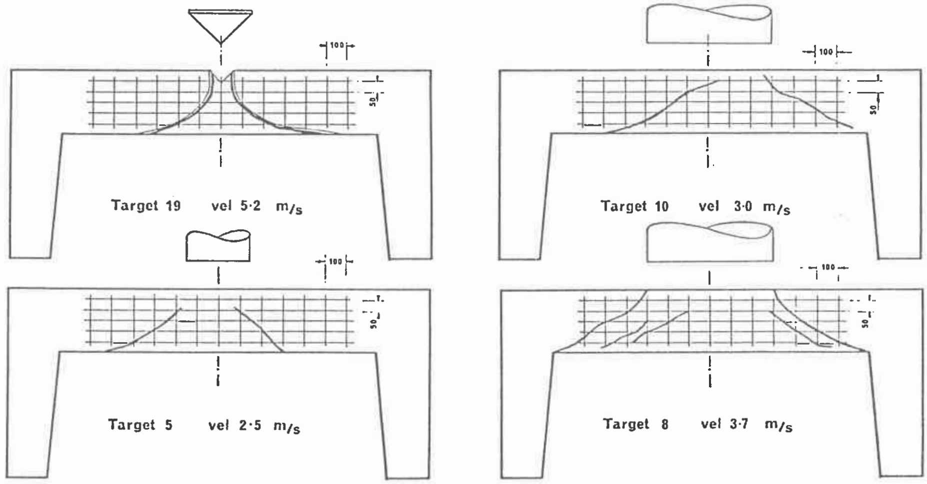

Figure 2 Target sections showing cone cracking

failure surface formed.

That such a minimum size is required has been noted by Jowett /3/, who showed with a simple model that cone crack formation rather than concrete crushing occurs when

$$\frac{\text{Contact diameter}}{\text{Slab thickness}} > \frac{1}{2.7}$$

This was confirmed for target 19, where this ratio was 1/2.8.

With the assumption that the energy of the impactor is primarily absorbed during the initial crushing stage of the impact event by plastic deformation, the deceleration a of impactor mass m is given as

(2) $a = A\,\sigma'/m$

at any given time, where A is the contact area at that time and σ' is the dynamic compressive strength.

Figure 3 shows the result from impactor and slab rear accelerometers for the 90° cone impact, Target 19. The peak deceleration during the crushing phase ($460 m/s^2$) and contact diameter (107mm) give

(3) $\sigma' = 3.3 f_{cy}$

A simplified model thus sees the impact event proceeding in three stages. Stage 1 is concrete crushing, absorbing energy E_{cr}. Stage 2 is the formation of the cone crack, creating a plug of concrete beneath the impactor and absorbing energy E_{cc}. Stage 3 is the knock-on of this plug with deformation of the reinforcing bars and consequent plug fragmentation. This absorbs the residual energy E_r and brings the impactor to rest in knock-on distance k.

With impact kinetic energy E_i, indentation depth h, and neglecting elastic energy in the target, there is a simple energy balance,

(4) $E_i + mgh = E_{cr} + E_{cc} + E_r$

It is hypothesised that each right-hand term varies as f_{cy} and hence results may be normalized to 32 MPa, the nominal strength. Thus E_{cr} is

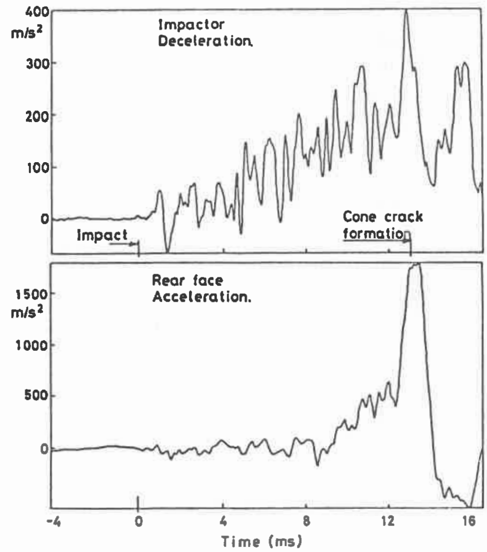

Figure 3 Acceleration for 5.2 m/s impact of 90° cone

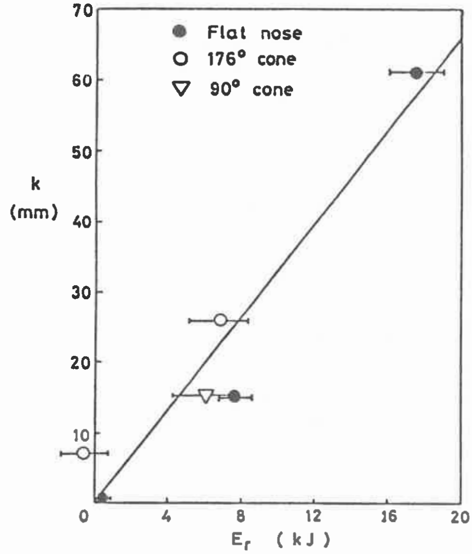

Figure 4 Dependence of plug knock-on on residual energy

the product of crushed volume and σ' (proportional to f_{cy} by eq. (3)), E_{cc} is determined by the crack geometry and concrete tensile strength ($\sim$0.15 f_{cy}), and the residual energy E_r is expected to be primarily dissipated in the fragmentation of the concrete plug.

The knock-on distance k of the plug would be expected to be some function, as yet unknown, of the residual energy E_r. Figure 4 shows that, for the limited data available, k varies linearly with normalised E_r. The Figure confirms the choice of 7200J (2.4 m/s velocity for the 2500 kg impactor) as the critical energy (and velocity) for cone crack formation with the flat-nose.

With crushing energy given as 106 MJ/m^3, the critical velocity for the 90° cone nose would be 4.4 m/s.

It will be seen from Table I that the formula derived from the NDRC data for scabbing of the rear face concrete considerably overestimates the velocity at which significant local damage arises.

5.2 PERFORATION

The results of Table I show that perforation of the slab occurred at velocities below that expected from eq. (1), with deviations varying between 15% and 35%. For the 300mm noses, the flat nose showed the greatest deviation. This was mitigated by the simulated 2° offset from parallelism of the 176° cone nose, and further mitigated by the 90° cone nose which represents corner impact.

With the same reinforcement B but with reduced bar diameter and mesh size, a worthwhile improvement in impact resistance was obtained (target 21). Further, the presence of front-face reinforcement significantly reduced indentation.

It is tempting to manipulate the method for calculating B to achieve agreement between prediction and observation. Thus setting B = 0.215% (i.e. halving the original calculation) gives an almost perfect answer for the 600mm flat-nose and improves the deviation for the 300mm flat-nose. Nevertheless a much fuller database is required together with a fuller understanding of the impact energy absorption. This will give the necessary theoretical basis for assessing floor safety under the variety of dropped loads that may be postulated.

Finally we note that the form of eq. (1), in its B dependence, cannot be appropriate for dropped loads. Thus for an B=0 we would expect

$$V_p = V_{cc}$$

since once the cone failure surface had formed, no further resistance to perforation would be possible. In our case V_p from eqn. (1) would be 7.2 m/s for the 300mm impactor, much exceeding V_{cc} = 2.4 m/s.

6 CONCLUSIONS

The series of tests reported here has necessarily investigated only a limited range of parameter variations. Firm conclusions require additional test work. Interim results are:

1. Rear face scabbing, as for example used in the NDRC prediction, is not relevant, and the scabbing formula is not conservative in predicting significant local damage.
2. As input velocity increases, a through-thickness cone crack marks initial significant local damage with the loss of leak-tightness.
3. With a flat-nosed impactor damage initiated at 2.4 m/s.
4. When exposed to "tilted" or "corner" impacts the concrete crushes as a shock absorber. The corresponding increase in the critical velocity for cone crack formation may be calculated using a dynamically enhanced crushing strength.
5. There is a limit to the shock absorbing capacity, by reason of a maximum contact region before the cone crack forms. The ratio of contact diameter to slab thickness is of order 2.8.
6. For the present slabs, reinforced on the rear face only and with target span to thickness ratio 5, perforation occurred at velocities below those predicted. The Deviation was up to 35%.
7. Improved perforation resistance was seen when

a) the mesh size was reduced, retaining the same reinforcement percentage.
b) the impactor had a cone nose (176° or 90° included angle) rather than presenting a "flat-on" impact.
c) the target had front face reinforcement, in addition to the standard reinforcement at the rear face.

REFERENCES

1 Fullard, K. and Barr, P. 1987. Development of design guidance for low velocity impacts. SMiRT-9, Paper J/5.
2 Wicks, S.J. 1987. Microconcrete model tests of heavy projectiles dropped from low heights. SMiRT-9, Paper J/2.
3 Jowett, J. 1986. The effects of hard missile impact on concrete. Lecture given to the Society for Earthquake and Civil Engineering Dynamics, London, 15/10/86.

This work was carried out at the Structural Test Centre, Cheddar, and Berkeley Nuclear Laboratories. This paper is published by permission of the Central Electricity Generating Board.